OK P

NASA TECHNICAL REPORT

NASA TR R-220

B058900

NASA TR R-220

ANALYSIS OF HEAT-TRANSFER EFFECTS IN ROCKET NOZZLES OPERATING WITH VERY HIGH-TEMPERATURE HYDROGEN

by John R. Howell, Mary K. Strite, and Harold E. Renkel

Lewis Research Center
Cleveland, Ohio

NATIONAL AERONAUTICS AND SPACE ADMINISTRATION • WASHINGTON, D. C. • FEBRUARY 1965

NASA TR R-220

ANALYSIS OF HEAT-TRANSFER EFFECTS IN ROCKET NOZZLES OPERATING WITH VERY HIGH-TEMPERATURE HYDROGEN

By John R. Howell, Mary K. Strite, and Harold E. Renkel

Lewis Research Center
Cleveland, Ohio

NATIONAL AERONAUTICS AND SPACE ADMINISTRATION

For sale by the Office of Technical Services, Department of Commerce,
Washington, D.C. 20230 -- Price $2.00

ANALYSIS OF HEAT-TRANSFER EFFECTS IN ROCKET NOZZLES OPERATING WITH VERY HIGH-TEMPERATURE HYDROGEN

by John R. Howell, Mary K. Strite, and Harold E. Renkel

Lewis Research Center

SUMMARY

An analytical technique suitable for the solution of complex energy transfer problems involving coupled radiant and convective energy transfer is developed. Solutions for the coupled axial wall energy flux distribution in rocket nozzles using hydrogen as a propellant are presented. Flow rates and temperatures studied are near those forecast for gaseous-core nuclear-propulsion systems. Parameters varied are nozzle shape, inlet propellant temperature, mean reactor cavity temperature, and nozzle wall temperature level. The effects of variation of the propellant radiation absorption coefficient with pressure, temperature, and wavelength are presented, and real property variations are used where they appear to be significant. Comparison is made to a simplified, coupled solution using a modified second-order one-dimensional diffusion equation for the radiative transfer.

At the temperature levels assumed, radiative transfer may account for a greater portion of the total energy transfer over important portions of the nozzle, and its effects cannot, therefore, be neglected.

Extreme energy fluxes (near 3×10^8 Btu/(hr)(sq ft)) are observed for certain cases, and this implies that new nozzle cooling techniques must be developed.

INTRODUCTION

With the advent of advanced nuclear-propulsion systems such as the gaseous-core configuration, extremely high propellant temperatures are expected. Propellant temperatures encountered in the nozzles of such systems may exceed 15,000°, leading to the belief that radiative energy transfer in the nozzle may be of significant importance in comparison with convective heat transfer. The purpose of this report is the investigation of the relative importance of these modes of energy transfer at the temperature levels expected and the development of a suitable analytical method for examing them.

Thermal design of a nozzle depends on knowledge of the axial heat-flux

distribution at the nozzle wall. The flux at any point along the nozzle is composed of convective and radiative contributions. The convective heat transfer is affected by variations in propellant enthalpy, viscosity, Prandtl number, Mach number, specific heat ratio, and molecular weight, each of which is, in turn, a function of local conditions. Radiative energy transfer is dependent on the distribution of propellant spectral absorption coefficient for radiation, which is dependent on the local static temperature and pressure distribution throughout the nozzle. Both radiative and convective energy transfer are coupled to the propellant flow. All of these factors are also geometry dependent.

Robbins (ref. 1) and Robbins, Bachkin, and Medeiros (ref. 2) studied the thermal design of a nozzle in conjunction with a solid-core nuclear reactor. Both papers considered radiant transfer between surfaces within the nozzle, but the propellant was assumed to be transparent, and absorption and emission of radiant energy in the propellant were therefore neglected. Coupling between radiant and convective heat transfer in the propellant does not occur in this case. Grueber (ref. 3) studied a nozzle cooled solely by radiation but also assumed the propellant transparent. For some propellants, notably hydrogen, assumption of transparency at the temperature levels considered previously (below 6000° R) is good; however, it becomes progressively poorer as the temperature levels increase.

Convective heat transfer in rocket nozzles has received considerable attention because it is the dominant heat-transfer mode in the systems widely used today. Representative papers are those of Bartz (refs. 4 and 5), Fortini and Ehlers (ref. 6), Benser and Graham (ref. 7), and Welsh and Witte (ref. 8).

Neumann and Bettinger (ref. 9) examined the major accepted methods of computing the gas-side convective heat-transfer coefficients in solid-core nuclear-rocket systems and demonstrated the effects of many variables on the predicted convective heat flux.

Of interest, when the coupling of radiation with flow is considered, are a number of analyses limited chiefly by their restriction to simple geometries and constant properties. Some of those that most closely approximate the problems studied herein are as follows: Einstein (refs. 10 and 11) obtained heat-transfer rates and temperature distributions between semi-infinite plates and in circular ducts containing flowing gases. He considered the effects of flow, conduction, and radiation in the gray absorbing-emitting medium, and included internal energy generation as a parameter. Chen (ref. 12), using an approximate formulation, was able to study radiation-scattering effects under similar conditions between semi-infinite plates.

Kramer (ref. 13) examined combined convective and radiative transfer for use in an analysis of transpiration cooling, but he considered the propellant to be a "black" gas radiating as a black surface directly to the nozzle wall and did not include coupling between radiation and convection. No consideration was given to the high-temperature reactor chamber or its contribution of radiant energy to the nozzle.

Howell, Strite, and Renkel (ref. 14) analyzed a specific nozzle shape for the coupled convective and radiative transfer. The first paper was restricted to constant propellant properties with a cursory examination of convective effects, while the second included variations in propellant properties.

This report examines in detail the radiative contribution to the total axial heat-flux distribution in a nozzle. Property variations and their effect on the radiative and convective heat flux and radiation from the upstream reactor chamber are taken into account.

SYMBOLS

A_i area of nozzle wall bounding increment i, sq ft

A_x cross-sectional area of nozzle, sq ft

B convergence control constant

C_g energy per bundle, Btu

$C_{p,i}$ heat capacity of propellant evaluated at conditions in increment i, Btu/(lb)($^\circ$R)

D local nozzle diameter, ft

e_λ Planck spectral distribution of emissive power, Btu/(sq ft)(hr)(ft)

$F_E(R)$ radial emission function at nozzle entrance, ft

$\mathscr{F}$ radiation exchange factor

H propellant enthalpy, Btu/lb

h_i nozzle wall heat-transfer coefficient in increment i, lb/(hr)(sq ft)

i axial increment index

j radial increment index

k dummy axial increment index

L path length between radiating and absorbing element, ft

l actual bundle path length, ft

M local propellant Mach number

m dummy radial increment index

N	net rate of energy bundles entering nozzle, bundles/hr
n	bundle index for radiant source
P_i	static pressure in increment i, lb/sq ft
Pr	propellant Prandtl number
p	bundle index for flow source
Q	rate of radiant energy entering nozzle from reactor chamber, Btu/hr
R	number chosen at random from set of numbers evenly distributed in range 0 to 1
R^*	local radius of nozzle, ft
r	radial position from nozzle axis of bundle at end of path, ft
rad	square of radial bundle position at end of path, r^2, sq ft
S	rate of bundle absorptions in nozzle wall increment, bundles/hr
$S(i,j)$	rate of bundle absorptions in propellant increment (i,j), bundles/hr
T	temperature, ^{o}R
$U(i,j)$	rate of bundle emissions due to flow sources in increment (i,j), bundles/hr
V	volume, cu ft
W	total propellant mass-flow rate, lb/hr
W_j	propellant mass-flow rate in increment j, lb/hr
w	molecular weight
x	coordinate perpendicular to nozzle axis (taken through bundle origin), ft
y	coordinate perpendicular to x and z, ft
z	axial coordinate, ft
α_i	angle between nozzle wall and nozzle axis at increment i
β	program index: 0 for radiant source segment, 1 for flow source segment

Γ $(x^2 + y^2)$ where x and y are computed at position of interest, sq ft

γ propellant ratio of specific heats

δ desired percentage temperature change between iterations

η angle measured clockwise from x around z

κ spectral propellant radiation absorption coefficient, ft^{-1}

$\bar{\kappa}$ mean propellant radiation absorption coefficient, ft^{-1}

λ wavelength, ft

μ propellant viscosity, lb/(ft)(hr)

ξ radiation path length in volume element dV, ft

σ Stefan-Boltzmann constant, 1.714×10^{-9} Btu/(hr)(sq ft)($^{\circ}R^4$)

Subscripts:

ad adiabatic

a,e absorbing or emitting element

$\not{c}$ centerline

ch chamber

conv convective

d truncated at decimal point

g gas

i evaluated in increment i

in inlet

i,j evaluated in increment i, j

j evaluated in increment j

max maximum

min minimum

n	nozzle
new	results of current iteration
o	evaluated at origin
rad	radiated portion
ref	evaluated at reference condition
s	static condition
st	stagnation
t	evaluated at nozzle throat
w	wall
λ	wavelength dependent

METHOD OF ANALYSIS

The analytical method consists of writing an energy balance on each volume element of propellant within the nozzle shown in figure 1 and solving the re-

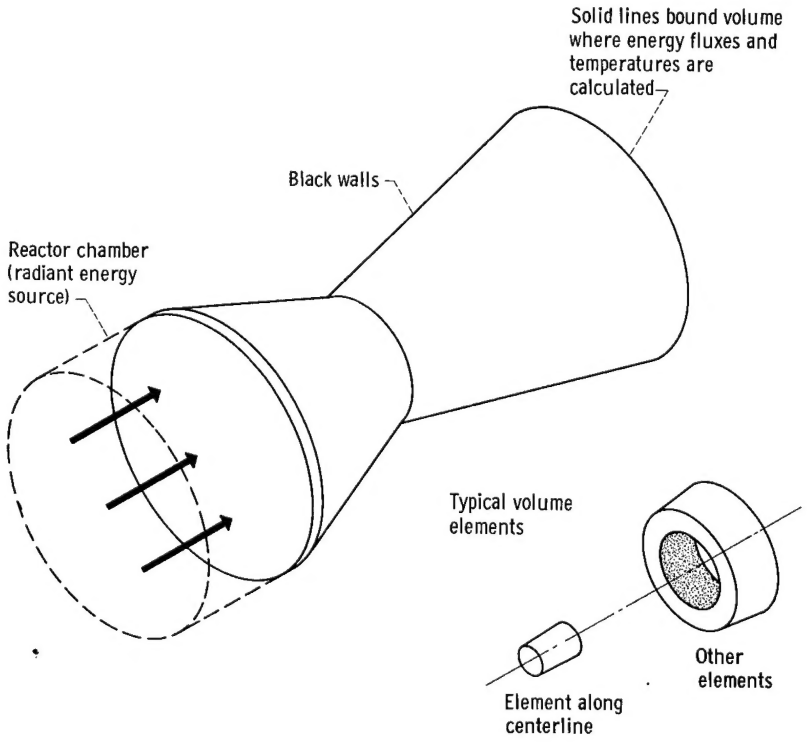

Figure 1. - Model for nozzle heat transfer.

sultant set of nonlinear second-order integro-differential equations. A typical equation from this set and a discussion of the detailed technique used in the solution are given in appendix A.

A complete flow scheme showing the application of these equations to a digital computer program is given in appendix B. A discussion of computer running time and program convergence is included.

In brief, the method of solution involves evaluation of the integrals implicit in the equations by a Monte Carlo technique. A new axial total temperature distribution is then found by solving the set of simultaneous equations by the Newton-Raphson method as presented in reference 15. The axial static temperature distribution is then computed and used to find local properties. This prodedure is repeated until convergence of the temperature distribution. Axial heat-flux distributions are then computed on the basis of this temperature profile.

Assumptions

In order to make the analysis tractable, the following assumptions are made:

(1) The nozzle walls are perfect absorbers for all incident radiation.

(2) No energy is added to the propellant by radiant emission from the nozzle walls.

(3) The radiation absorption coefficient in the propellant does not vary along the path between the points of energy emission and absorption, and its value is based on local conditions at the point of emission.

(4) A one-dimensional isentropic analysis is adequate to describe the Mach number and the static pressure distributions in the nozzle.

(5) Equilibrium physical properties can be used at local conditions.

(6) Gamma heating of the propellant and the nozzle walls can be ignored.

(7) Complete radial mixing occurs within the nozzle, so that there are no radial temperature gradients.

(8) No net flow crosses one-dimensional streamlines within the nozzle.

These assumptions and their validity are discussed in appendix A.

Features of Method

Incorporation of the Monte Carlo technique to evaluate the radiation terms allows freedom from the common transparent or constant absorption coefficient propellant assumptions and further allows a reasonably straightforward analysis

of the coupling between radiation and convection. The complete solution technique allows consideration of most variations of physical properties with temperature and pressure where these variations appear important. As finally programmed for the digital computer, these effects plus those of nozzle geometry, mass flow rate and mass flow rate distribution, reactor cavity radiation, and nozzle wall temperature distribution can be investigated.

Diffusion Solution

A much more straightforward, but also more restricted, solution to the nozzle heat-transfer problem can be obtained by modifying the second-order diffusion solution as presented by Deissler (ref. 16) for the radiative portion of the problem and combining this with the pipe flow equation for convection. The assumptions involved and the method of modification used to obtain these equations are given in appendix C.

It is possible to obtain a solution by hand with this method, whereas a high-speed digital computer is mandatory for the Monte Carlo solution. Neither the effects of thermal radiation from the nuclear-reactor cavity nor the spectral effects, however, are conveniently studied by the one-dimensional radiation diffusion approach used herein.

Determination of the heat transfer is obtained by iterative solution of the equation

$$T_i = T_{i-1} - \frac{A_i}{WC_{p,i}} \left[\frac{\sigma(T_s^4 - T_w^4)_i}{\left(\frac{3\bar{K}D}{16} + \frac{9}{8\bar{K}D} + \frac{1}{2} \right)_{i-(1/2)}} + h_i(H - H_w)_i \right] \tag{1}$$

starting with volume element $i = 1$. Solution for this element gives an initial guess for element $i = 2$, and this procedure is continued along the nozzle length.

The axial heat-flux distribution is then obtained from

$$\left(\frac{Q}{A} \right)_i = \frac{WC_{p,i}}{A_i} \left(T_{i-1} - T_i \right) \tag{2}$$

DESCRIPTION OF PROBLEM ANALYZED

The problem solved by the methods presented is the heat-transfer rate as a function of axial position for a conical nozzle. The propellant is assumed to be hydrogen. The effects of nozzle shape, radiation absorption coefficient, inlet propellant temperature, apparent reactor cavity temperature, variable

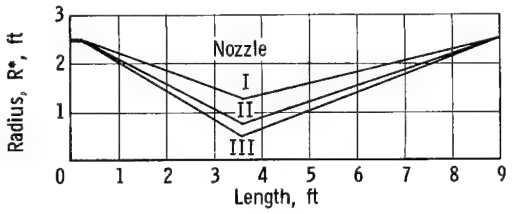

Figure 2. - Dimensions of nozzles.

TABLE I. - MASS FLOW RATES OF HYDROGEN FOR VARIOUS NOZZLE SHAPES

[Entering propellant static pressure, 100 atm.]

Nozzle	Inlet temperature, T_{in}, ^{o}R	
	13,000	15,000
	Mass flow rate of hydrogen, lb/sec	
I	940	---
II	350	320
III	153	---

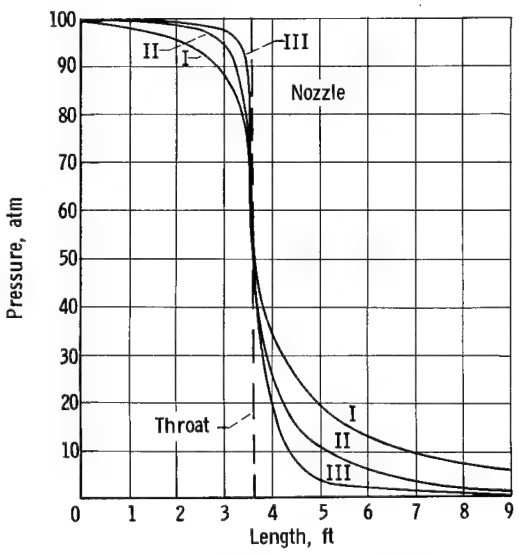

Figure 3. - Nozzle pressure distributions.

nozzle wall temperature, and the coupling of radiation and convection will be demonstrated.

The effects of a number of parameters on the axial distribution of energy flux to the walls of a nozzle are presented. For each nozzle shape examined (fig. 2), the flow rate of propellant was taken as that producing sonic flow at the throat on the basis of the one-dimensional isentropic flow equations. These flow rates are shown in table I. The nozzle shapes and sizes were chosen as representative of those anticipated for gaseous-core nuclear systems.

Propellant enthalpy, viscosity, heat capacity, ratio of specific heat, and radiation absorption coefficient were allowed to vary in the manner noted in appendix C for all the results presented. On the basis of the one-dimensional flow assumption, the propellant is divided into volume elements; typical ones are shown in figure 1.

Pressure and Mach number distributions calculated from standard isentropic flow equations are assumed sufficiently accurate and are shown in figures 3 and 4, respectively, for the nozzle shapes studied. Except for the figure showing the effect of wall temperature, all calculations are based on a constant nozzle wall temperature of 4000^{o} R.

RESULTS AND DISCUSSION

General Remarks

A cursory examination of figures 5 to 11 shows that the shape of the axial energy flux distribution in the nozzle is similar for all cases where radiation and convection are considered simultaneously. A large peak in total flux, reaching values near 2×10^{8} Btu/(hr)(sq ft), occurs at the nozzle throat because of the increased mass-flow rate per unit area.

The total flux drops rapidly downstream

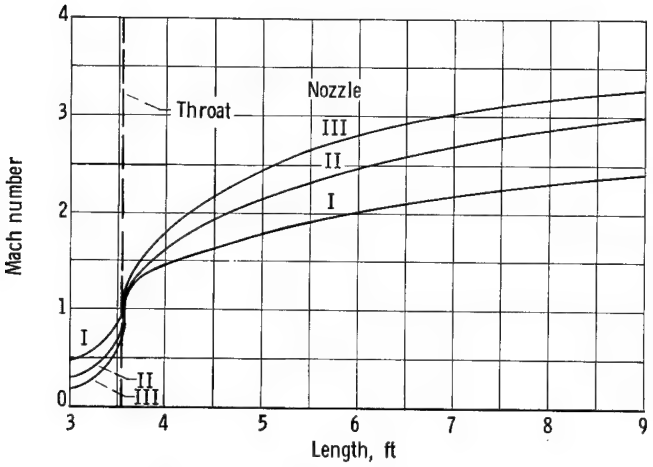

Figure 4. - Nozzle Mach number distributions.

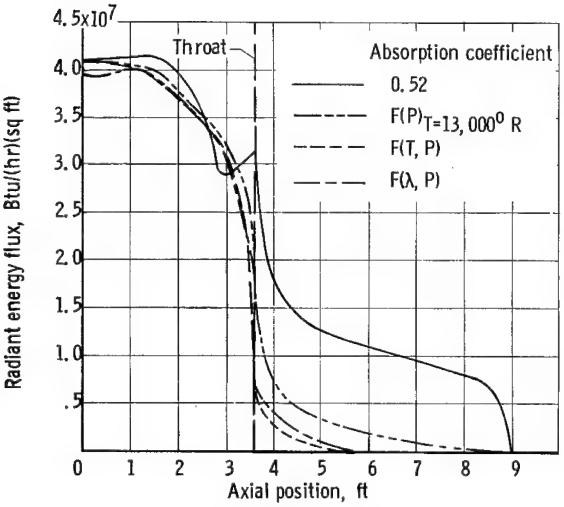

Figure 5. - Effect of radiation absorption coefficient on total radiant energy flux. Nozzle, II; chamber temperature, 13,000° R; inlet temperature, 13,000° R; wall temperature, 4000° R.

of the throat because of a number of interrelated effects. The total propellant temperature has decreased slightly because of upstream heat losses, and the propellant static temperature is also lowered rapidly at points further downstream because of the increasing propellant Mach number. Both of these effects tend to lower the convective heat transfer.

The radiative transfer, which can be quite significant upstream of the nozzle throat, also decreases rapidly downstream of the throat. This is because the fourth power of the static temperature is decreasing rapidly, and the hydrogen propellant becomes nearly transparent at the lower static conditions downstream of the throat. Both factors tend to radically decrease the radiative transfer. Radiation contributes from under 5 to nearly 90 percent of the total flux depending on the case under consideration.

Effect of Variation of Radiation Absorption Coefficient

Figure 5 demonstrates the effects on the radiative energy flux of certain assumptions about the variation of propellant absorption coefficient with local conditions. While the constant mean absorption coefficient chosen predicts a greater radiative transfer, the other assumptions lead to results that are in fair agreement except in the divergent section where radiation effects are small. This was the basis for computing most of the results by using only the simplest variation, that is, with static pressure. The assumption of variation with both static temperature and pressure predicted the lowest radiative transfer rate as expected from the property variations for this system shown in figure 4. Since each variation examined lowered the computed flux from that found for a constant coefficient, consideration of variation with all three (static temperature, pressure, and wavelength) simultaneously would be expected to predict even smaller radiant fluxes.

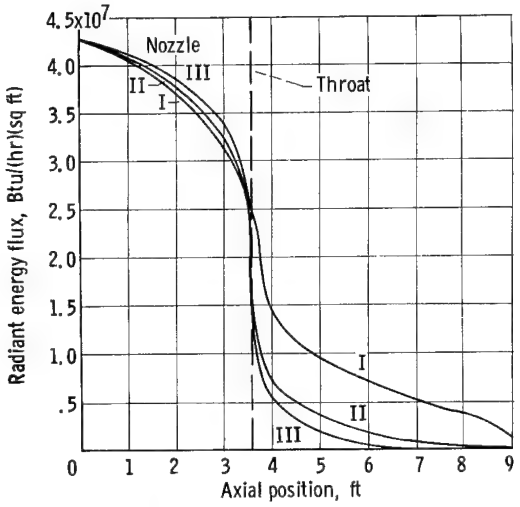

Figure 6. - Effect of nozzle shape on independent radiant flux to nozzle. Inlet temperature, 13,000° R; reactor temperature, 13,000° R; wall temperature, 4000° R; $\bar{\kappa} = F(P)_{T=13,000^\circ R}$.

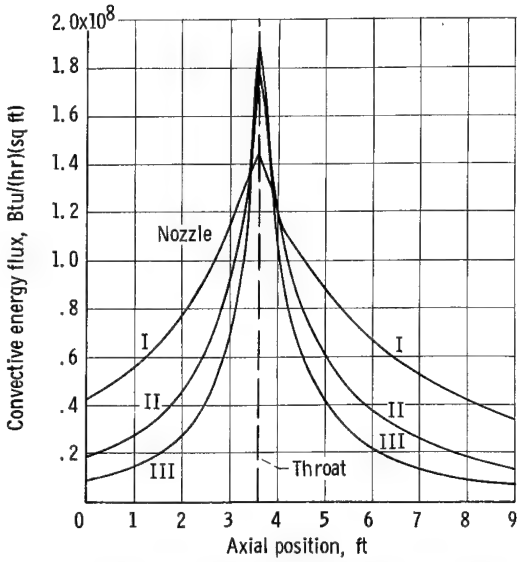

Figure 7. - Independent convective flux to nozzle. Inlet temperature, 13,000° R; wall temperature, 4000° R.

Effect of Nozzle Shape on Flux Distribution

In figure 6, the radiant flux is shown with the nozzle shape as a parameter. Here the absorption coefficient is assumed to be dependent only on local static pressure. Since it has the largest throat diameter and, therefore, the smallest convergence angle, nozzle I has the smallest static pressure and temperature drop. This in turn causes it to have the highest radiative flux past the throat because the absorption coefficient remains comparatively high, as does the local static temperature. In addition, geometric shielding is less. On the other hand, the higher Mach number and lower local static temperature and pressure at a given axial location upstream of the throat in nozzle I results in a comparatively lower local radiative flux in this part of the nozzle.

Figure 7 indicates the effect of nozzle shape on the convective heat transfer. Nozzle III has the smallest throat diameter and, thus, the greatest convergence angle and the smallest flow rate of propellant. This causes the convective flux in the convergent and divergent portions of nozzle III to be smaller than that in the other nozzles. At the throat, however, nozzle III exhibits the largest heat flux; this is due to the effect of the large mass-flow rate per unit area on the heat-transfer coefficient.

Effect of Considering Total Heat Flux as Additive or Coupled

The radiative fluxes of figure 6 and the convective fluxes of figure 7 were computed independently. However, because each heat-transfer mechanism tends to lower the total propellant temperature, which in turn affects the static temperature and the properties, there is some question as to whether simply adding the results will accurately predict the total heat transfer. The computer program is written to consider the two modes of heat transfer

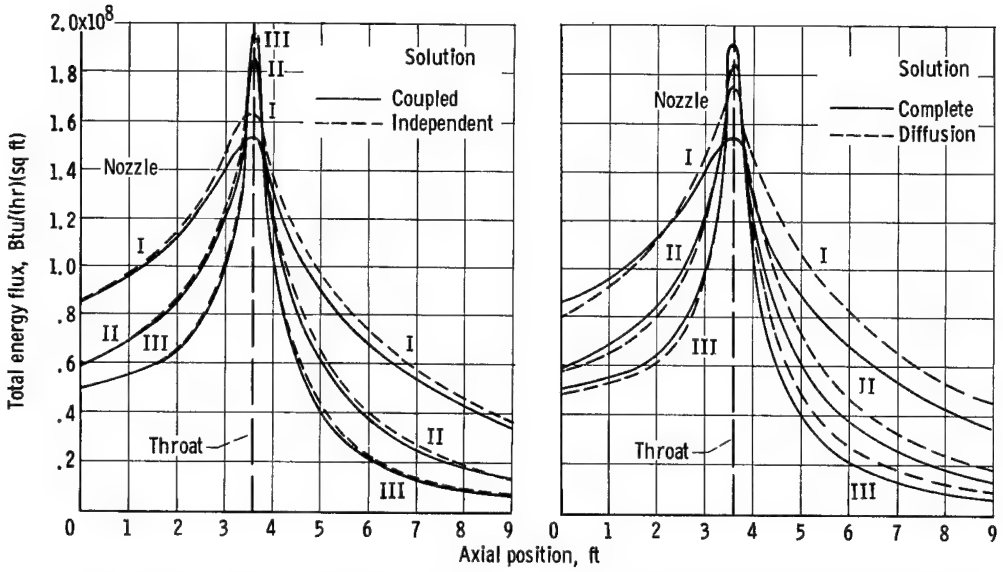

(a) Comparison of coupled and independent solutions. Chamber temperature, 13,000° R; inlet temperature, 13,000° R; wall temperature, 4000° R.

(b) Comparison of coupled and diffusion solutions.

Figure 8. - Comparison of total energy flux. $\bar{\kappa} = F(P)_{T=13,000^\circ R}$.

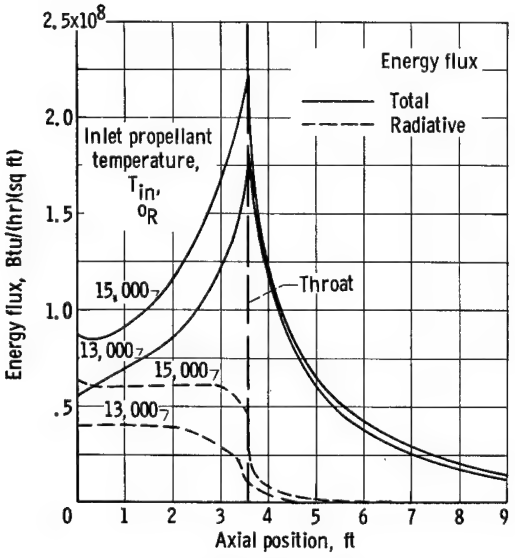

Figure 9. - Effect of inlet propellant temperature on radiative and total coupled energy flux. Nozzle, II; $T_{ch} = T_{in}$; wall temperature, 4000° R; $\bar{\kappa} = F(P)_{T_{in}}$.

as coupled, and this is done in the remainder of the figures.

Figure 8(a) shows the differences in the total energy fluxes obtained by adding the radiative and convective fluxes and those resulting from calculating the coupled effect. The additive solutions are seen to slightly overpredict the total flux, because each is based on a propellant temperature distribution that is somewhat too high. Since the energy loss in the propellant stream is relatively small at the large flow rates present in these nozzles, the total temperature of the stream remains almost unchanged no matter which method is used in calculating the heat transfer. The use of coupled calculations for the specific cases presented herein is, therefore, not necessary, since an additive method produces acceptable accuracy.

Comparison With Solution by Radiation Diffusion Method

Comparison of the more complete solution is made with the second-order diffusion solution with jump boundary conditions of reference 17 and modified as described in appendix C. The diffusion results (fig. 8(b)) presented are based

on the assumption that the radiation is proportional to the fourth power of the total temperature of the propellant rather than the static temperature, and use a pressure dependent Rosseland mean radiation absorption coefficient (see appendix C) taken from reference 17. Propellant heat capacity was allowed to vary with pressure, but the propellant ratio of specific heats was taken as constant and equal to 1.0. This caused neglect of the effects of static temperature variation due to acceleration of the propellant.

Convection was computed as for the more complete solution. Comparison of the solutions for similar cases is shown in figure 8(b). As expected, the more complete solution gives more accurate values of energy flux upstream of the throat because the energy entering from the upstream reactor chamber is considered. Downstream of the throat, the diffusion solution overpredicts the flux because variations of the static temperature were neglected. Aside from these effects, agreement is surprisingly good. For certain cases, especially where large effects of the reactor chamber thermal radiation are present, less agreement would be expected.

Effect of Inlet Propellant Temperature

Figure 9 demonstrates the effect of two propellant temperatures at the nozzle inlet on the total coupled energy flux. As expected, the flux is much greater at the higher propellant temperature. Two factors mainly account for this. They are the increased temperature level of the propellant which increases the radiant flux, and the larger enthalpy difference between the propellant and the wall, which increases the convective flux. Another factor is the property variations that occur with temperature; in most cases, the property variations lend an additional increase to the energy flux at higher temperatures, although variations in the heat capacity and ratio of specific heats are so complex as to forestall a definite statement in their cases.

Effect of Reactor Chamber Temperature Level

The upstream reactor chamber may have a large effect on the nozzle heat transfer through its thermal radiation contribution. Figure 10(a) demonstrates the magnitude of possible variation, based on a number of mean reactor chamber temperatures. The radiative contribution to the energy flux becomes so large for high reactor chamber temperatures that the peak flux occurs at the nozzle entrance rather than the throat, and a severe cooling problem appears at this rather unexpected area.

Since the reactor radiation acts as an energy source, the propellant temperature is expected to change locally for different reactor temperatures. Figure 10(b) indicates that the stagnation temperature of propellant within the nozzle may increase because of this effect.

Because of the possible wide variation between the temperatures of the major emitting (reactor chamber) and absorbing (nozzle propellant) portions of the system, spectral effects could become important. Assuming the propellant properties to be independent of wavelength leads to the differences in calcu-

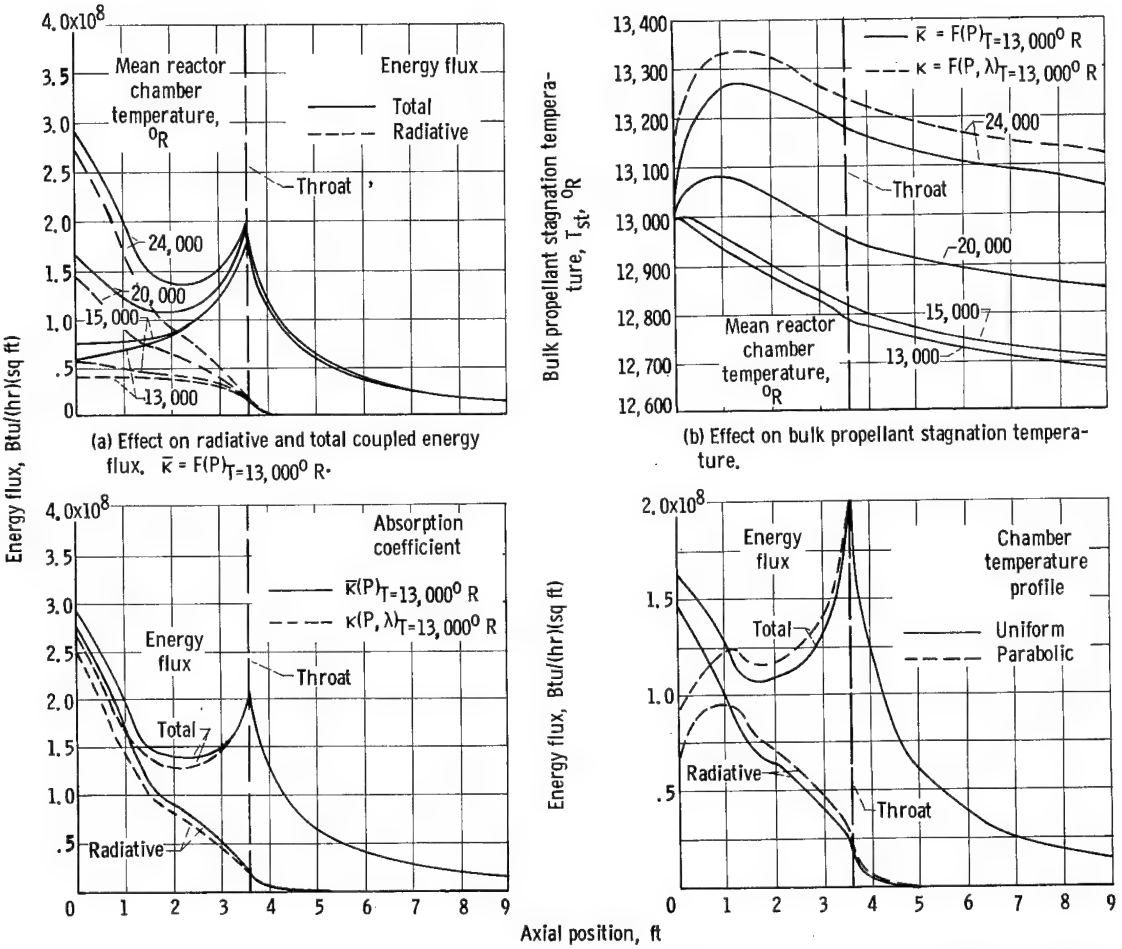

(a) Effect on radiative and total coupled energy flux. $\bar{\kappa} = F(P)_{T=13,000^0\ R}$.

(b) Effect on bulk propellant stagnation temperature.

(c) Effect of spectral absorption coefficient on radiative and total coupled energy flux. Chamber temperature, 24,000° R.

(d) Effect of reactor chamber temperature distribution on radiant energy flux.

Figure 10. - Effect of reactor chamber temperature. Nozzle, II; inlet temperature, 13,000° R; wall temperature, 4000° R.

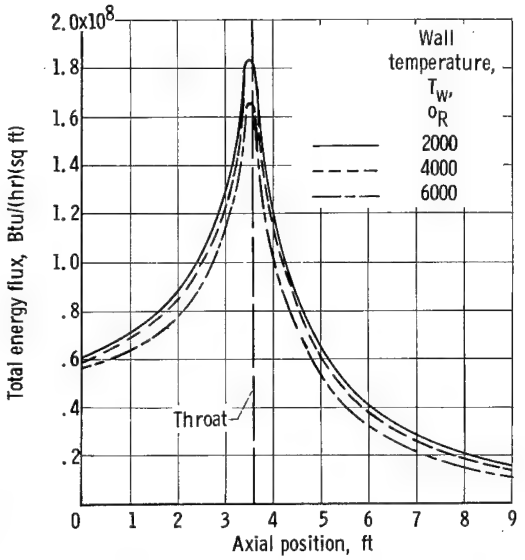

Figure 11. - Effect of nozzle surface temperature on total coupled energy flux. Nozzle, II; chamber temperature, 13,000° R; inlet temperature, 13,000° R; $\bar{K} = F(P)_{T=13,000^\circ R}$.

lated propellant temperature shown in figure 10(b). As the wavelength effect increases the propellant temperature, more energy must be absorbed by the propellant than for the wavelength independent case. This implies that less energy will reach the nozzle walls for the spectral case, and this conclusion is borne out by the results presented in figure 10(c).

Effect of Reactor Chamber Temperature Distribution

Figure 10(d) shows the effect of nonuniformity in the radial temperature distribution in the reactor cavity. The solid lines show the energy flux profiles for a constant reactor cavity temperature of 20,000° R, while the dotted lines are the profiles for a parabolic temperature distribution in the reactor cavity that radiates the same total energy as in the constant temperature case. This distribution had a peak temperature at the nozzle centerline of 24,000° R and a minimum at the nozzle wall of 15,000° R. A significant reduction in the peak radiative flux at the nozzle wall is evident, indicating that the distribution of entering energy is important.

Effect of Nozzle Surface Temperature

The nozzle surface temperature is a relatively weak parameter (fig. 11). A large (4000° R) change in the surface temperature produces only a relatively small variation in energy flux.

CONCLUDING REMARKS

An analytical method for determining the axial distribution of coupled radiative and convective energy flux on a rocket nozzle wall is introduced. The method consists of using a Monte Carlo technique for finding the radiative transfer in conjunction with a standard matrix solution routine for the set of governing equations. Speed of convergence and attainable accuracy in solving a nozzle heat-transfer problem is found to be good.

The results of the analysis for cases representative of anticipated conditions in a nozzle used with a gaseous-core nuclear-propulsion system are presented. The magnitude of the fluxes computed reach extremely high levels and, for some cases, is near 3×10^8 Btu/(hr)(sq ft). This value is more than thirty times higher than the peak values computed by Benser and Graham (ref. 7) for a representative large nozzle in a chemical-rocket using hydrogen-oxygen propellant.

to p. 16

These high fluxes may occur near the nozzle entrance and are, therefore, effective over a relatively large area of the nozzle wall, in contrast to chemical rockets where the peak flux occurs only over a relatively small area near the throat. This implies extreme heat loads to any nozzle coolant system.

The effect on the flux of increased wall temperature is so small that nozzle materials with higher temperature capabilities will be of little value in solving the cooling problem. Some results indicate that consideration of radial temperature profiles may reduce computed peak wall fluxes.

The flux at the nozzle wall due to either convection or radiation is of such magnitude as to demand cooling methods involving film cooling, transpiration, boundary-layer seeding, or possibly elimination of a physical nozzle and use of electromagnetic effects.

Lewis Research Center
National Aeronautics and Space Administration
Cleveland, Ohio, November 12, 1964

APPENDIX A

ANALYSIS

Method of Solution

For a general volume element dV with axial position index i and radial position index j, by using the assumptions listed in the section Assumptions, an energy balance gives

$$\underset{\downarrow}{\mathscr{A}} \qquad\qquad \underset{\downarrow}{\mathscr{B}}$$

$$\left(\begin{array}{l}\text{Energy radiated into } dV_{i,j} \\ \text{from other propellant elements} \\ \text{and the reactor cavity}\end{array}\right) + (\text{Flow energy entering } dV_{i,j}) =$$

$$\underset{\downarrow}{\mathscr{C}} \qquad\qquad\qquad\qquad\qquad\qquad \underset{\downarrow}{\mathscr{D}}$$

$$(\text{Energy radiated from } dV_{i,j}) + (\text{Flow energy leaving } dV_{i,j})$$

$$\underset{\downarrow}{\mathscr{E}}$$

$$+ (\text{Energy lost to nozzle wall from } dV_{i,j}) \qquad (A1)$$

This can be written mathematically by substituting the following relations:

$$\mathscr{A} = \int_{\lambda} \left[\kappa_a \int_{V_n} 4\, \mathscr{F}_{e-a}\, \kappa_e e_{g,\lambda} \exp\left(-\int_0^L \kappa\, dL\right) dV \right.$$

$$\left. + \int_{A_n} e_{w,\lambda} \mathscr{F}_{w-a} \exp\left(-\int_0^L \kappa\, dL\right) dA_w \right] d\lambda\, d\xi$$

$$\mathscr{B} - \mathscr{D} = \left(WC_p \frac{\partial T}{\partial z}\, dz\right)_{i,j}$$

$$\mathscr{C} = 4 \int_{\lambda} \kappa_a e_{g,\lambda}\, dV_{i,j}\, d\lambda$$

$$\mathscr{E} = \left[h_i A_{w,i} (H_i - H_{w,i})\right]_j$$

The index of refraction of the propellant is taken as constant and equal to 1.0 and therefore does not appear in the radiation terms.

Solution of equation (A1) for the total temperature of the volume element is desired, because, knowing this, the energy flux to the wall can be found. Solution of this equation, however, demands a complete knowledge of the propellant temperature distribution for evaluation of the integral terms. Because of this and the temperature dependence of many of the physical properties, an iterative procedure must be used. A total temperature distribution T(i) is assumed and is used to evaluate the static temperature distribution that is used, in turn, to evaluate the temperature dependent properties. The set of equations for all (i,j) is then solved simultaneously by the Newton-Raphson method (ref. 15) to obtain a new total temperature distribution. This distribution is used as the new guess to determine a static temperature distribution for evaluating properties, and the procedure is continued until the assumed and computed temperature distributions agree within prescribed limits.

Solution of the equations is greatly complicated by the presence of term $\mathscr{A}$ in equation (A1). Some further simplifications must be made to make an evaluation of the integral terms tractable. One desirable simplification, if it is justifiable in the case under discussion, is to consider κ constant along the path L between the radiating and absorbing element even though it remains dependent on the static temperature and pressure of the radiating element. Under this restriction the exponential terms inside the integrals reduce to $\exp(-\kappa_e L)$ where κ_e is a function of the local conditions in the emitting element.

Term $\mathscr{A}$, thus modified, can be evaluated by a Monte Carlo technique. This technique consists of dividing the energy emitted by each radiating volume or area into finite bundles, and following each bundle through its lifetime of absorptions and emissions until final loss from the enclosed nozzle volume. This loss can occur by means of the bundle passing through the entrance or exit, by absorption at the nozzle wall and, in some cases, in propellant flow sinks. Derivation of the functional relations governing the events along the paths of these bundles is given in reference 18 with a discussion of application to radiant energy transfer problems.

Discussion of Assumptions

Obviously, limitations are placed on the accuracy of the analysis by the assumptions made. The effect of many of the assumptions depends on the specific nozzle and propellant studied.

Convective and radiative energy is assumed to be removed from each radial element in proportion to the radial distribution of flow. This corresponds to the case of complete radial mixing when a one-dimensional flow is assumed.

The total temperature is computed solely on the basis of heat-transfer effects; the lowering of total temperature due to friction is neglected. In the divergent portion of the nozzle, therefore, the radiation and convection from

the propellant will be somewhat overpredicted.

A constant radial temperature is assumed on the basis of the large flow rates and mixing anticipated in such systems. Little information is available on radial mixing for nozzle geometries, and the validity of this assumption cannot be assessed.

A further assumption is that the propellant radiation absorption coefficient is a function of at most two variables: either (1) local propellant static temperature and pressure or (2) wavelength and local propellant static pressure. It is, in principle, possible to include the variation of absorption coefficient with wavelength together with the effects of temperature and pressure. However, computer running time would be significantly increased by the addition of another variable, so the program was limited to variations only in the combinations noted. For any propellant, the assumption of the absorption coefficient being invariant between the point of emission and the point of absorption becomes valid if any of the following criteria are met: (1) Conditions throughout the nozzle vary only slightly. (2) Distances between regions at different conditions are large compared to the radiation mean free path (the reciprocal of the absorption coefficient). (3) The absorption coefficient is a weak function of local conditions. (4) The geometry is such that points under widely different conditions cannot see one another. Under these conditions, either the mean absorption coefficient will be nearly constant throughout the nozzle or radiant energy will be blocked or greatly attenuated before reaching a region with a different absorption coefficient.

Under conditions (1) and (3), neglect of variation of the absorption coefficient with wavelength, static pressure, or static temperature also becomes quite a good assumption. Variations from these restrictions, of course, add increasing uncertainty to the magnitude of the errors involved. For hydrogen propellant in a nozzle studied in the example herein, these assumptions are met quite well. This is because the major part of the radiative transfer occurs in the portion of the nozzle upstream of the throat where static pressure and temperature variations are small due to the relatively small changes in Mach number. This, in turn, causes the local property variations in this region to be small. The downstream portion of the nozzle, where variations in propellant absorption coefficient can be significant due mainly to large variations in local static conditions, contributes little radiant energy to the upstream section because of the blocking effect of the convergent-divergent geometry.

Since the inlet propellant temperatures studied are above $10{,}000^{\circ}$ R and the nozzle wall temperature is below 6000° R, the radiant energy contributed to the system by the wall is negligible in comparison with the energy entering from the reactor cavity and that originating in the propellant. For this reason, no energy is considered to be originating at the nozzle wall for the propellant heat balance even though an emission term is included in the energy balance used to determine the net wall heat flux.

To account for energy radiated into the nozzle from the reactor cavity, the assumption is made that, in the plane normal to the nozzle axis, the radiant energy enters diffusely, that is, follows the cosine law. The amount of

radiation entering the nozzle from the reactor chamber must be specified. For a spectral solution, the spectral energy distribution is taken to be that of a black body at the mean reactor chamber temperature.

The exhaust plume of the nozzle is assumed to be transparent to radiation on the basis of the mean absorption coefficient data for hydrogen shown in figure 4 and, therefore, neither absorbs nor emits radiation. Because nuclear propulsion will in general be used only in space, no radiation from atmospheric interactions is considered.

For computing the value of the convective heat-transfer coefficient, the method presented by Benser and Graham (ref. 7) was chosen as being relatively simple to use while being reasonably accurate. The definition of reasonably accurate is somewhat nebulous in this case since no experimental data is available under the conditions imposed; however, at lower temperatures, experimental comparison seems adequate (ref. 6) for a similar analysis.

Use of a possibly more accurate but definitely much more complex boundary-layer analysis for the convective heat transfer does not seem justified for this work. Certainly the pipe-flow equation as modified should accurately reflect the effects of parametric variations in the significant variables.

Benser and Graham (ref. 7) suggest the use of an enthalpy difference heat-transfer coefficient given by the following equation:

$$h = \frac{0.026\left(\frac{W}{A_x}\right)^{0.8} \mu_{ref}^{0.2}}{D^{0.2}\, Pr_{ref}^{0.667}} \left(\frac{\frac{T_s}{w}}{\frac{T_{ref}}{w_{ref}}}\right)^{0.8} \qquad \text{lb/(hr)(sq ft)} \qquad \text{(A2)}$$

with the properties evaluated at a reference enthalpy given by

$$H_{ref} = H_s + 0.5\,(H_w - H_s) + 0.22\, Pr_{ref}^{1/3}\,(H - H_s)$$

The convective heat flux is then given by

$$\left(\frac{Q}{A_w}\right)_{conv} = h(H_{ad} - H_w)$$

where

$$H_{ad} = H_s + Pr_{ref}^{1/3}\,(H - H_s)$$

The coefficient, 0.026, in equation (A2) is an arbitrary value that has been shown experimentally to vary with the axial position in the nozzle. Such variation must be determined experimentally for a specific nozzle and specific conditions and was therefore taken as constant herein. The value 0.026 is suggested in reference 7.

APPENDIX B

COMPUTER PROGRAM

The simplified flow chart given by figure 12(a) shows in a general form the computer approach followed in the determination of the nozzle heat-flux distribution. The major sections of the program are expanded to give a complete flow chart in the subsequent parts of figure 12.

Running time for the program varied widely. As finally modified and programed using the Fortran IV compiler on an IBM 7094 digital computer, complete running times for a single case averaged much less than 10 minutes. This varied depending on the astuteness of the original guess of propellant temperature distribution, the magnitude of property variations in the static pressure and temperature range under consideration, the accuracy of solution required, and a number of other interrelated factors. The Monte Carlo segment of the program was the largest time consumer, and the time used was especially dependent on the number of energy bundles followed and the propellant opacity.

Accuracy of the solutions is almost impossible to bracket analytically in an iterative Monte Carlo solution tied to other finite difference program segments. A discussion of this is given in reference 19. Lacking such an analytical estimate, however, it is nevertheless possible to deduce the error by more prosaic means.

For these solutions, accuracy could be determined by comparison to known limiting solutions, such as for pure convection or pure radiation. The latter was done in reference 14 for this type of program, and the former is presented herein by figures 7 and 8. Also, comparison is made in figure 8(b) with an independent total solution. These comparisons give confidence that convergence to the correct solutions is being obtained.

Confidence that fully converged solutions are presented is gained by increasing the number of volume increments in the nozzle and/or increasing the number of Monte Carlo energy bundles followed. If the answers do not change, which they did not for the cases checked, then it is probable that full convergence is present.

It was found that 20 axial and 5 radial increments gave sufficient accuracy. Convergence under any set of conditions was assumed present if no temperature in the entire distribution changed by more than 0.1 percent between iterations. This took three to four iterations for most cases.

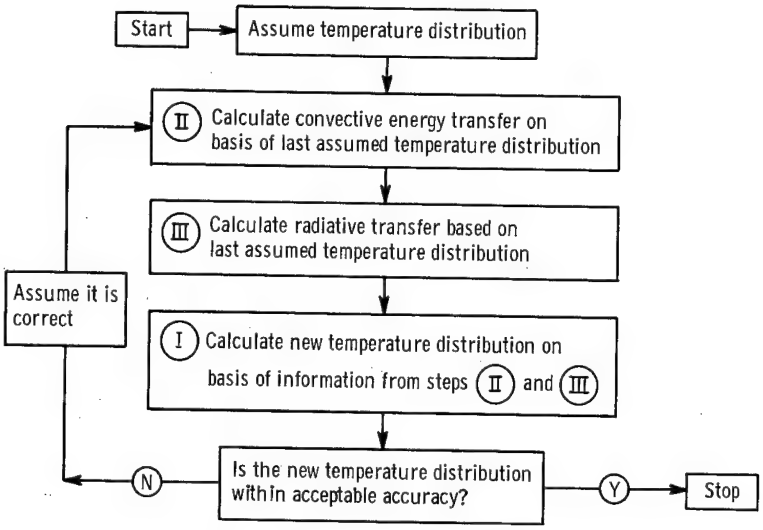

(a) Schematic outline.

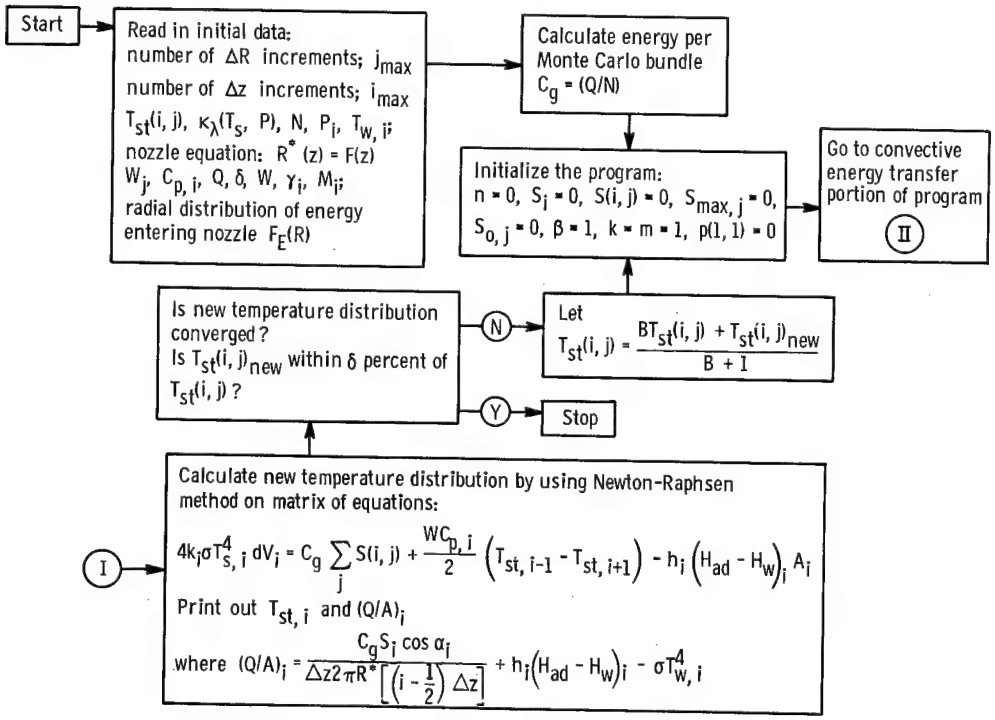

(b) Part I.

Figure 12. - Computer flow scheme.

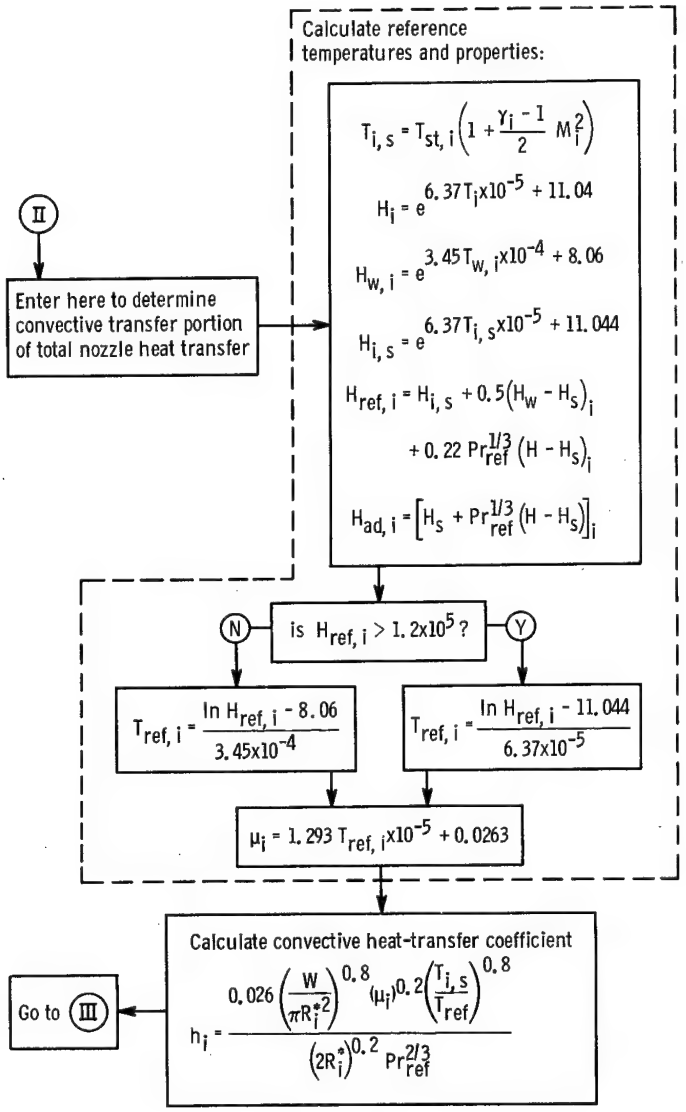

(c) Part II.

Figure 12. - Continued. Computer flow scheme.

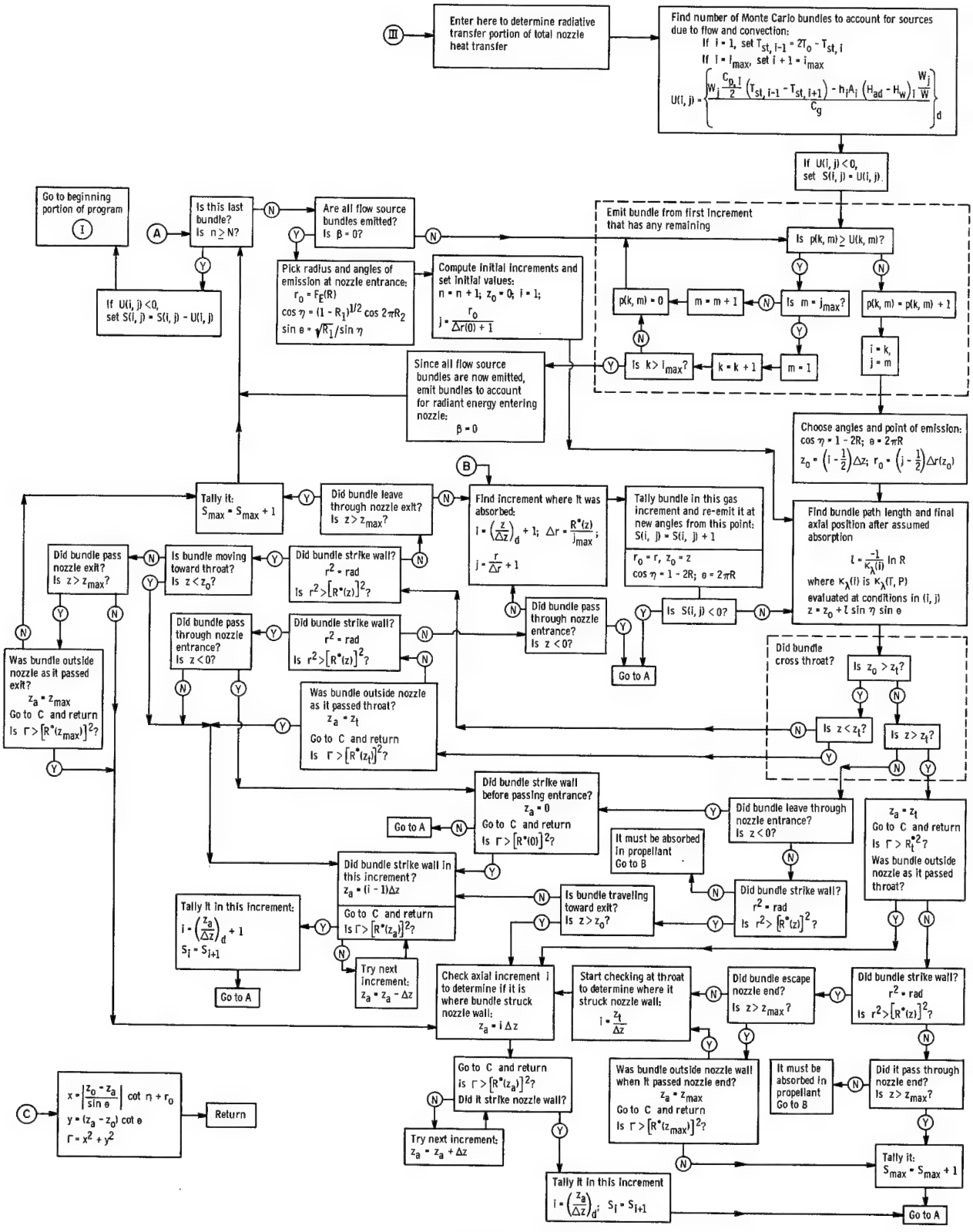

(d) Part III.

Figure 12. - Concluded. Computer flow scheme.

APPENDIX C

DIFFUSION SOLUTION

Deissler (ref. 16) has derived equations for the temperature distributions and wall heat-transfer rates due to radiation in infinitely long cylinders. Under the assumption of a gray gas flowing in a black tube, his equation (43) reduces to

$$\left(\frac{Q}{A}\right)_{rad} = \frac{\sigma\left(T_{\ell}^4 - T_w^4\right)}{\frac{3\bar{K}D}{16} + \frac{9}{8\bar{K}D} + \frac{1}{2}} \tag{C1}$$

This was derived using a second-order diffusion solution incorporating the effects of the radiative emissive power discontinuity that occurs at the cylinder boundary. The Rosseland mean absorption coefficient defined by

$$\frac{1}{\bar{K}} = \int_0^{\infty} \frac{1}{K_\lambda}\left(\frac{\partial e_{g,\lambda}}{\partial e_g}\right) d\lambda$$

must be used in this equation.

Use of the discontinuity in emissive power at a solid boundary as a radiation boundary condition is questionable in the present case. This effect actually occurs only in a model in which there is no conduction of energy and would be hard to realize physically. However, the sharp gradient appearing between the bulk propellant temperature and the wall temperature across the boundary layer at any point along the nozzle wall provides a physical situation at least approximating this condition, and the assumption of a jump radiation boundary condition may be justified here.

This equation was adapted for use in the nozzle by assuming that the propellant temperature at the nozzle centerline T_{ℓ}, the absorption coefficient $\bar{K}$, and the tube diameter D are all evaluated at the axial position of interest. In addition, radiant wall flux is evaluated on the basis of the area of each tapering nozzle wall element, rather than the cylindrical elements used in reference 17. For the equation to be valid under these conditions, the propellant must be optically dense enough that radiation effects up- and downstream of the point under consideration do not appreciably affect that point. This condition can only be tested by comparison to more exact solutions, but the results will probably be poor near both the exit and entrance of the nozzle.

The total heat transfer to some wall element i will be made up of radiative and convective energy, so that

$$\frac{Q}{A} = \left(\frac{Q}{A}\right)_{rad} + h_i(H - H_w) \tag{C2}$$

Loss of this energy to the wall will cause a temperature drop in the propellant given by

$$\left(\frac{Q}{A}\right)_i = \frac{WC_{p,i}(T_{i-1} - T_i)}{A_i} \tag{C3}$$

Substituting equations (C3) and (C1) into equation (C2) gives

$$T_i = T_{i-1} - \frac{A_i}{WC_{p,i}} \left[\frac{\sigma\left(T_s^4 - T_w^4\right)_i}{\left(\frac{3\bar{K}D}{16} + \frac{9}{8\bar{K}D} + \frac{1}{2}\right)_{i-(1/2)}} \right] + h_i(H - H_w)_i \tag{C4}$$

where

$$A_i = \frac{\Delta z \ \pi D_i}{\cos \alpha_i}$$

$$\alpha_i = \tan^{-1}\left(\frac{D_{i-1} - D_i}{2\Delta z}\right)$$

and Δz is the axial length of the element considered.

Equation (C4) can then be solved for T_{i-1} if T_o, the inlet propellant temperature, is given. T_1 is used to solve for T_2, and this procedure is used to generate the axial propellant temperature profile. Equation (C2) is then used to determine the axial wall heat-flux distribution.

APPENDIX D

HYDROGEN PROPERTIES

Equilibrium physical properties used were taken from a number of sources and examined for their dependence on static temperature and pressure.

Values of both enthalpy and radiation absorption coefficient were taken from reference 17.

The values of the radiation absorption coefficient given in reference 17 are spectral. Examination of these values shows a variation of one to three orders of magnitude over the spectrum of interest at any temperature and pressure encountered in the nozzles investigated, with larger variations in relatively low pressure, low temperature regions. The Planck mean absorption coefficient, defined by

$$\bar{\kappa} = \frac{\int_{\lambda_{min}}^{\lambda_{max}} \kappa_\lambda e_{g,\lambda} d\lambda}{\int_{\lambda_{min}}^{\lambda_{max}} e_{g,\lambda} d\lambda}$$

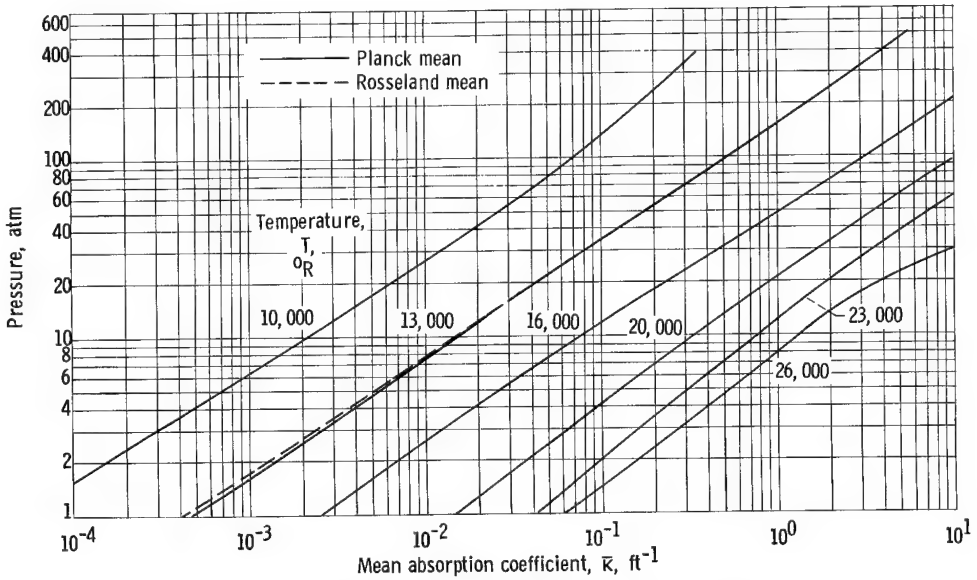

(a) Mean equilibrium radiation absorption coefficient of hydrogen. (Data taken from ref. 17.)

Figure 13. - Hydrogen radiation absorption coefficient.

where $e_{g,\lambda}$ is the Planck black body energy distribution, shows a variation of many orders of magnitude over the range of either pressure or temperature expected. This type of mean results from consideration of radiation in gases that have negligible self-absorption (see ref. 16). The computed values of the Planck mean absorption coefficient are shown in figure 13(a), and spectral values for various pressures at a temperature of 13,000° R are shown in figure 13(b). Because of the magnitudes of the changes with pressure, temperature, and wavelength, all these variables should be examined. However, accurate consideration of the three variables simultaneously requires a complex interpolation routine and storage of large amounts of data, making a very unwieldly program. Variation in a combination of two variables was used, as noted in appendix A.

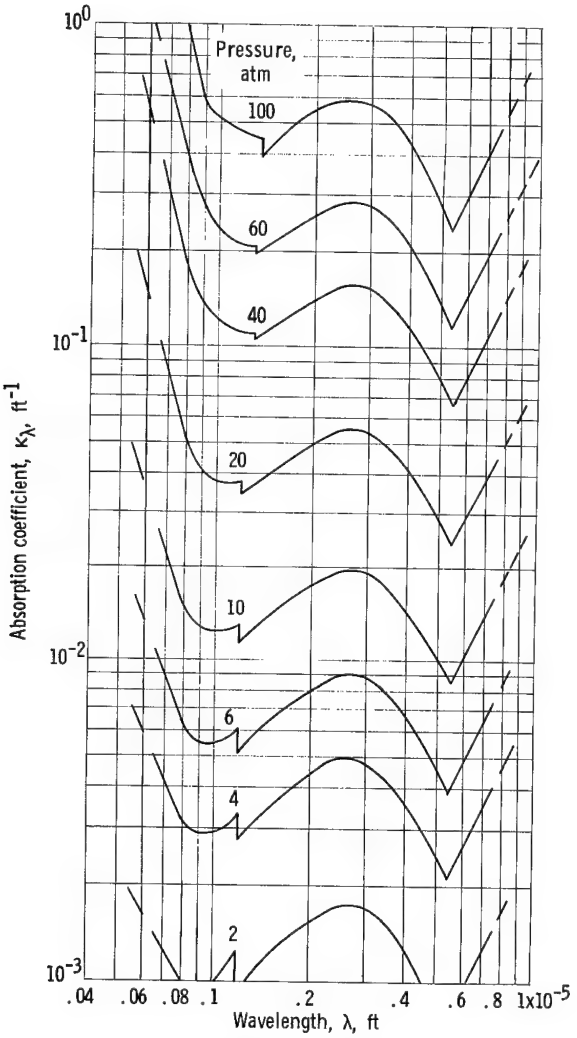

(b) Spectral absorption coefficient for hydrogen gas at 13,000° R. (Data taken from ref. 17.)

Figure 13. - Concluded. Hydrogen radiation absorption coefficient.

Enthalpy data for hydrogen is shown in figure 14. Since variations with pressure are small in comparison with temperature variations, the data was approximated by the dotted lines in figure 14. These are given by the relations

$$H = e^{3.45\ T_s \times 10^{-4}} + 8.06 \quad \text{Btu/lb}$$

$$\text{for } T_s \leq 10{,}000^\circ \text{ R} \qquad \text{(D1)}$$

$$H = e^{6.37\ T_s \times 10^{-5}} + 11.044 \quad \text{Btu/lb}$$

$$\text{for } T_s > 10{,}000^\circ \text{ R} \qquad \text{(D2)}$$

Heat-capacity data are taken from reference 20 and are shown in figure 15. Variations with both temperature and pressure are large, and neither is neglected. Hydrogen viscosity data are also from reference 20 and are plotted in figure 16. Variations with pressure are small, especially at high temperatures, and the viscosity is approximated by

$$\mu = 1.293\ T_s \times 10^{-5} + 0.0263$$

$$\text{lb/(ft)(hr)} \qquad \text{(D3)}$$

Prandtl number data from reference 20, show only small variations with temperature and pressure and so the Prandtl number was assumed constant at a value of $Pr = 0.65$.

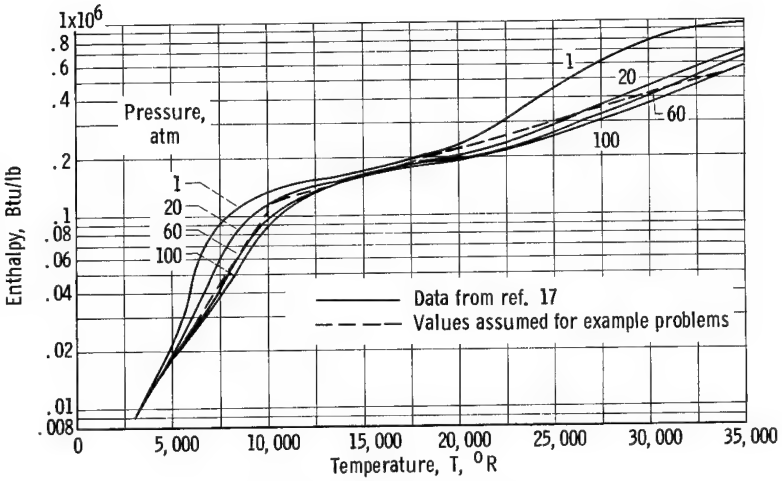

Figure 14. - Enthalpy of hydrogen gas.

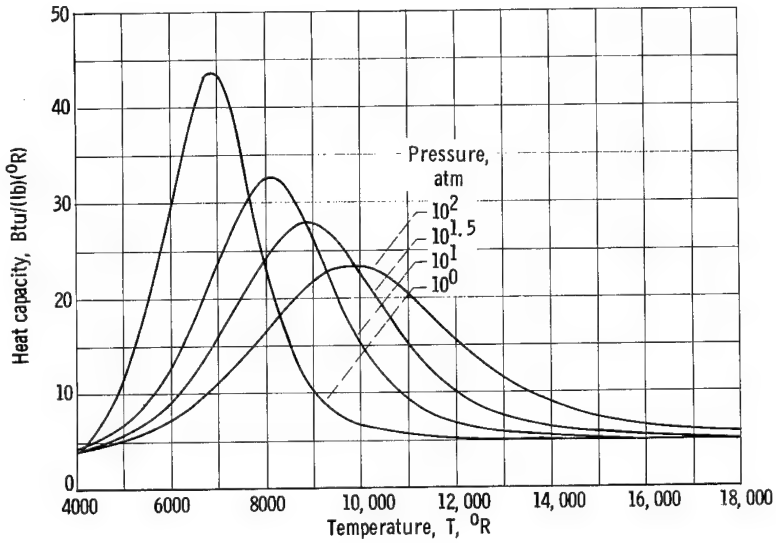

Figure 15. - Equilibrium heat capacity of hydrogen gas. (Data taken from ref. 20.)

Molecular weight and ratio of specific heat data are found in references 20 and 21. The molecular weight does not vary significantly under the conditions expected and, since it appears as a ratio to a fractional exponent in equation (A2) its variation is assumed to have negligible influence.

The specific-heat ratio, needed to calculate static conditions, varies widely with both temperature and pressure, and the curves shown in figure 17 are used.

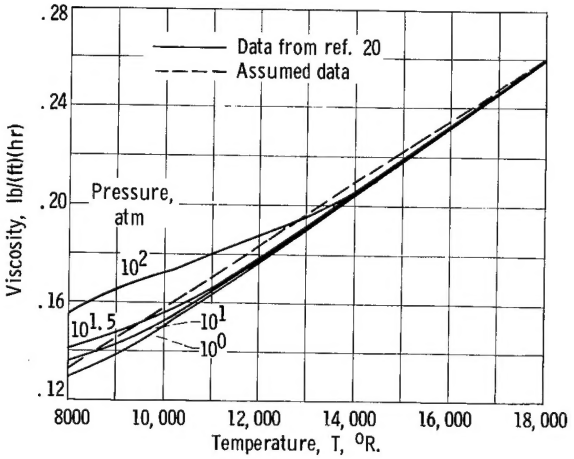

Figure 16. - Viscosity of hydrogen gas.

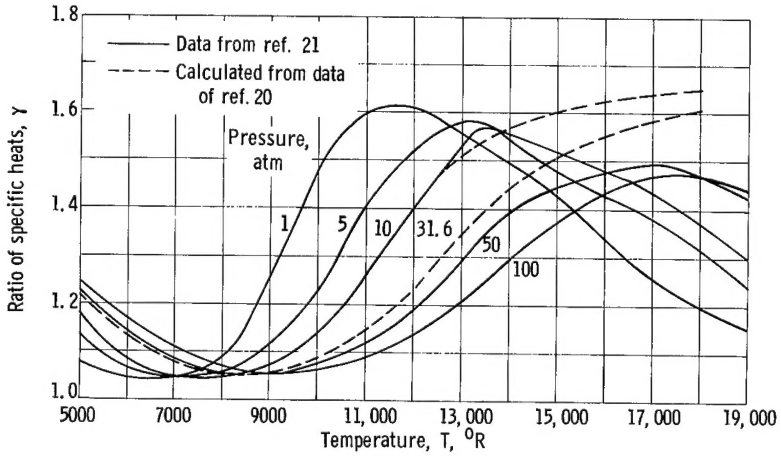

Figure 17. - Equilibrium ratio of specific heats for hydrogen gas.

REFERENCES

1. Robbins, William H.: An Analysis of Thermal Radiation Heat Transfer in a Nuclear-Rocket Nozzle. NASA TN D-586, 1961.

2. Robbins, William H., Bachkin, Daniel, and Medeiros, Arthur A.: An Analysis of Nuclear-Rocket Nozzle Cooling. NASA TN D-482, 1960.

3. Grueber, Gerald: A Method of Calculating Wall Temperatures in a Radiation-Cooled Rocket Nozzle. Rep. R-002, Aerojet-General Corp., Mar. 9, 1962.

4. Bartz, Donald R.: An Approximate Solution of Compressible Turbulent Boundary-Layer Development and Convective Heat Transfer in Convergent-Divergent Nozzles. Trans. ASME, vol. 77, no. 8, Nov. 1955, pp. 1235-1245.

5. Bartz, Donald R.: A Simple Equation for Rapid Estimation of Rocket Nozzle Convective Heat Transfer Coefficients. Jet Prop., vol. 27, no. 1, Jan. 1957, pp. 49-51.

6. Fortini, Anthony, and Ehlers, Robert C.: Comparison of Experimental to Predicted Heat Transfer in a Bell-Shaped Nozzle with Upstream Flow Disturbances. NASA TN D-1743, 1963.

7. Benser, William A., and Graham, Robert W.: Hydrogen Convective Cooling of Rocket Nozzles. Paper 62-AV 22, ASME, 1962.

8. Welsh, William E., Jr., and Witte, Arvel B.: A Comparison of Analytical and Experimental Local Heat Fluxes in Liquid-Propellant Rocket Thrust Chambers. Tech. Rep. 32-43, Jet Prop. Lab., C.I.T., Feb. 1, 1961.

9. Neumann, Harvey E., and Bettinger, Paula J.: A Comparative Analysis of Convective Heat Transfer in a Nuclear Rocket Nozzle. NASA TN D-1742, 1963.

10. Einstein, Thomas H.: Radiant Heat Transfer to Absorbing Gases Enclosed Between Parallel Flat Plates with Flow and Conduction. NASA TR R-154, 1962.

11. Einstein, Thomas H.: Radiant Heat Transfer to Absorbing Gases Enclosed in a Circular Pipe with Conduction, Gas Flow, and Internal Heat Generation. NASA TR R-156, 1962.

12. Chen, John C.: Simultaneous Radiative and Convective Heat Transfer in an Absorbing, Emitting, and Scattering Medium in Slug Flow Between Flat Plates. Rep. BNL 6876-R, Brookhaven Nat. Lab., Mar. 18, 1963.

13. Kramer, E. L.: Analysis of a Transpiration-Cooled Nozzle with Applications to a Gaseous Core Reactor. Rep. SM-44873, Douglas Aircraft Co., 1963.

14. Howell, John R., Strite, Mary Kern, and Renkel, Harold: Heat-Transfer Analysis of Rocket Nozzles Using Very High Temperature Propellants. NASA TP 14-63, 1963.

15. Ness, Arthur J.: Solution of Equations of a Thermal Network on a Digital Computer. Solar Energy, vol. 3, no. 2, 1959, p. 37.

16. Deissler, Robert G.: Diffusion Approximation for Thermal Radiation in Gases with Jump Boundary Condition. Jour. Heat Transfer (Trans. ASME) ser. C, vol. 86, no. 2, May 1964, p. 240.

17. Krascella, N. L.: Tables of the Composition, Opacity, and Thermodynamic Properties of Hydrogen at High Temperatures. NASA SP-3005, 1963.

18. Howell, John R., and Perlmutter, Morris: Monte Carlo Solution of Radiant Heat Transfer in a Nongrey Nonisothermal Gas with Temperature Dependent Properties. A.I.Ch.E. Jour., vol. 10, no. 4, July 1964, pp. 562-567.

19. Fleck, Joseph A., Jr.: The Calculation of Nonlinear Radiation Transport by Monte Carlo Method. Methods in Computational Physics, B. Alder, S. Fernbach, and M. Rotenberg, eds. Academic Press, pp. 43-65.

20. Grier, Norman T.: Calculation of Transport Properties and Heat-Transfer Parameters of Dissociating Hydrogen. NASA TN D-1406, 1962.

21. Ragsdale, Robert G.: Performance Capability of Single-Cavity Vortex Gaseous Nuclear Rockets. NASA TN D-1579, 1963.

NASA-Langley, 1965 E-2654

"The aeronautical and space activities of the United States shall be conducted so as to contribute . . . to the expansion of human knowledge of phenomena in the atmosphere and space. The Administration shall provide for the widest practicable and appropriate dissemination of information concerning its activities and the results thereof."

—NATIONAL AERONAUTICS AND SPACE ACT OF 1958

NASA SCIENTIFIC AND TECHNICAL PUBLICATIONS

TECHNICAL REPORTS: Scientific and technical information considered important, complete, and a lasting contribution to existing knowledge.

TECHNICAL NOTES: Information less broad in scope but nevertheless of importance as a contribution to existing knowledge.

TECHNICAL MEMORANDUMS: Information receiving limited distribution because of preliminary data, security classification, or other reasons.

CONTRACTOR REPORTS: Technical information generated in connection with a NASA contract or grant and released under NASA auspices.

TECHNICAL TRANSLATIONS: Information published in a foreign language considered to merit NASA distribution in English.

TECHNICAL REPRINTS: Information derived from NASA activities and initially published in the form of journal articles.

SPECIAL PUBLICATIONS: Information derived from or of value to NASA activities but not necessarily reporting the results of individual NASA-programmed scientific efforts. Publications include conference proceedings, monographs, data compilations, handbooks, sourcebooks, and special bibliographies.

Details on the availability of these publications may be obtained from:

SCIENTIFIC AND TECHNICAL INFORMATION DIVISION

NATIONAL AERONAUTICS AND SPACE ADMINISTRATION

Washington, D.C. 20546